

Highly Stable Water Splitting on Oxynitride TaON Photoanode System under Visible Light Irradiation

Masanobu Higashi,^{†,‡} Kazunari Domen,[§] and Ryu Abe^{*,†,‡}

[†]Catalysis Research Center, Hokkaido University, North 21, West 10, Sapporo 001-0021, Japan

[‡]JST-CREST, Sanbancho 5, Chiyoda-ku, Tokyo 102-0075, Japan

[§]Department of Chemical System Engineering, The University of Tokyo, 7-3-1 Hongo, Tokyo 113-8565, Japan

Supporting Information

ABSTRACT: Highly stable photoelectrochemical water splitting is demonstrated for the first time on a tantalum oxynitride (TaON) photoanode under visible light irradiation. Highly dispersed CoO_x nanoparticles on the TaON photoanode efficiently scavenge photogenerated holes and effectively suppress self-oxidative deactivation of the TaON surface, resulting in a stable photocurrent. The use of highly dispersed CoO_x cocatalyst on TaON together with phosphate solutions significantly increased the photocurrent due to the formation of a cobalt/phosphate phase. This enabled us to stably split water into H₂ and O₂ under visible light irradiation at a relatively low applied bias (0.6 V vs Pt counter electrode).

Photoelectrochemical and photocatalytic water splitting using semiconductors has attracted considerable attention due to the potential to produce H₂ from water by utilizing solar energy.^{1–4} The development of a stable semiconducting material that functions efficiently under visible light is essential to practically harness solar energy. Since oxide semiconductors generally possess high resistances to photocorrosion, visible-light-responsive oxides (e.g., WO₃,⁵ Fe₂O₃,⁶ and BiVO₄)⁷ have mainly been employed as photoanodes for water oxidation. However, it is essential to apply a relatively large external bias between the photoanode and counter electrode in these systems because the conduction band of these visible-light-responsive oxides is generally too positive for H₂ evolution. Applying a large external bias, using a power supply, is undesirable since it increases the overall energy consumption. Thus, it is desirable to develop a semiconductor that has both a sufficiently negative conduction band for H₂ production and a sufficiently narrow band gap (i.e., <3.0 eV) for visible light absorption. We previously reported that some metal oxynitrides, such as TaON,^{8,9} possess appropriate band levels for both water oxidation and reduction, and a narrow band gap that allows visible light absorption. The top of the valence band of these oxynitrides is much more negative than those of the corresponding oxides due to hybridization of the N 2p and O 2p orbitals. On the other hand, the bottom of the conduction band in these tantalum oxynitrides consists predominantly of empty tantalum orbitals. This results in energy levels similar to those of the corresponding metal oxide (Ta₂O₅), which are sufficiently negative for H₂ production. Consequently, some tantalum oxynitrides, such as TaON, are promising photo-

anodes, which have the potential to produce H₂ and O₂ from water under visible light irradiation with a relatively low (or even no) externally applied bias. However, the introduction of N 2p orbitals in the valence band generates a new problem in stability that needs to be solved. Most oxynitrides (e.g., TaON) undergo self-oxidative deactivation to some degree. In this reaction, photogenerated holes oxidize nitrogen anions (N³⁻) to N₂ (2N³⁻ + 6h⁺ → N₂).⁸ Because this self-oxidative deactivation proceeds competitively with water oxidation, the photocurrent of oxynitride photoanodes decreases rapidly on photoirradiation. We recently demonstrated that this problem can be solved to a certain extent by loading an effective cocatalyst for water oxidation, such as IrO_x on TaON photoanodes; the cocatalyst scavenges photogenerated holes and catalyzes water oxidation.^{10,11} However, loading the IrO_x cocatalyst did not completely suppress the reduction in both the photocurrent and the nitrogen content due to the poor dispersion of the nanoparticulate IrO_x cocatalyst on the TaON surface. Since holes in the bulk of n-type semiconductors generally have short diffusion lengths, it is essential to achieve a good dispersion of the water oxidation cocatalyst in order to efficiently scavenge holes and suppress self-oxidative decomposition. The present study reports the fabrication of a highly stable TaON photoanode that can efficiently generate O₂ under visible light irradiation at a relatively low applied potential. The cobalt-based cocatalyst nanoparticles are dispersed homogeneously on the surfaces of TaON particles.

TaON powder was prepared by our previously reported method.⁸ Co nanoparticles (5 wt%, calculated as metal) were loaded on TaON particles by impregnation from an aqueous Co(NO₃)₂ solution, followed by heating at 673 K for 30 min in air (referred to as CoO_x/TaON). As-prepared CoO_x/TaON particles were deposited on Ti substrate by electrophoretic deposition. The coated area was ca. 1.5 × 4 cm². The as-prepared electrodes were treated with 50 μL of TaCl₅ methanol solution (10 mM) and then dried in air at room temperature. After this process was performed five times, the electrode was heated in NH₃ flow (10 mL min⁻¹) at 723 K for 30 min (these represent the optimal heating conditions for fabricating CoO_x/TaON electrodes). Unloaded TaON electrodes were fabricated using almost the same procedure as above, except that the NH₃ treatment temperature was 823 K; they were then post-loaded

Received: March 1, 2012

Published: April 10, 2012

with cocatalysts. The resulting unloaded TaON electrode was treated with $\text{Co}(\text{NO}_3)_2$ or $\text{Na}_2[\text{IrCl}_6]$ methanol solution (Co, 5 wt%; Ir, 5 wt%), dried, and heated in NH_3 at 673 K for 30 min (referred to as $\text{CoO}_x(\text{post})/\text{TaON}$ and $\text{IrO}_x(\text{post})/\text{TaON}$, respectively). The electrochemical cell used in the photocurrent measurements consisted of a TaON electrode, a counter electrode (Pt wire), a Ag/AgCl reference electrode, and an electrolyte (0.1 M aqueous Na_2SO_4 or sodium phosphate buffer solution). The potential of the working electrode was controlled using a potentiostat. The electrodes were irradiated with light from a 300 W Xe lamp (LX-300F, Cermac) fitted with a cutoff filter (L-42, Hoya) to block light in the ultraviolet region. The irradiated area was ca. 6 cm^2 ($1.5 \times 4 \text{ cm}^2$). Detailed experimental conditions are given in the Supporting Information (SI).

The electronic state of the Co species loaded on TaON electrodes (CoO_x/TaON) was investigated by XPS (see Figure S1). Comparison of the main and satellite peaks of the Co species with those of standard samples (Co metal, CoO, and Co_3O_4) suggests that the prepared CoO_x/TaON electrodes predominantly contain Co^{2+} species. XRD analysis of CoO_x particles prepared directly from $\text{Co}(\text{NO}_3)_2 \cdot 6\text{H}_2\text{O}$ powder by heating in air at 673 K and subsequently in a NH_3 stream at 723 K indicates the formation of Co metal as the main species due to the reductive atmosphere of the NH_3 stream. This implies that CoO_x particles on the TaON electrode also contain Co metal species, which are readily oxidized on exposure to air. Interestingly, a characteristic current was observed at $\sim 0.6 \text{ V}$ vs RHE during the anodic scan in an aqueous Na_2SO_4 solution under visible light irradiation (see Figure S2), whereas no such current was observed during the anodic scan in the dark. This indicates that oxidation of Co species occurred photoelectrochemically during the anodic scan. XPS spectra of CoO_x/TaON electrode before and after the anodic scan under light irradiation suggest that some of the Co^{2+} species were oxidized to Co^{3+} . It can also be assumed that metallic Co species were oxidized to Co^{2+} . Since no such anodic current was observed after the second anodic scan, the current–potential curves obtained during the second anodic scan were used to evaluate the performance of the CoO_x/TaON photoanode. Figure 1A shows the current–potential relationship for CoO_x/TaON electrodes in aqueous Na_2SO_4 solution under chopped visible light irradiation ($\lambda > 400 \text{ nm}$). Although negligibly low photocurrent (below $10 \mu\text{A cm}^{-2}$ at 1.1 V vs

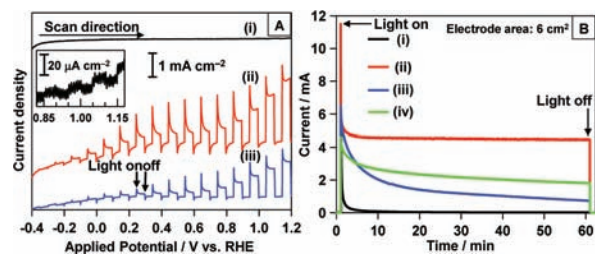


Figure 1. (A) Current–potential curves in aqueous 0.1 M Na_2SO_4 solution (pH 6) under chopped visible light irradiation ($\lambda > 400 \text{ nm}$) for (i) as-prepared CoO_x/TaON electrode, (ii) CoO_x/TaON electrode treated with TaCl_5 and NH_3 , and (iii) unloaded TaON electrode treated with TaCl_5 and NH_3 . (B) Time courses of the photocurrent of (i) unloaded TaON, (ii) CoO_x/TaON , (iii) $\text{CoO}_x(\text{post})/\text{TaON}$, and (iv) $\text{IrO}_x(\text{post})/\text{TaON}$ electrodes in aqueous 0.1 M Na_2SO_4 solution (pH 6) at 0.95 V vs RHE under visible light irradiation ($\lambda > 400 \text{ nm}$).

RHE) was observed for CoO_x/TaON deposited on a Ti substrate (Figure 1A-(i)), the CoO_x/TaON electrode subjected to post-necking treatment exhibited a clear photoresponse to visible light irradiation, as shown in Figure 1A-(ii). This is undoubtedly due to facilitated electron transfer between the TaON particles through the bridges formed during the post-necking treatment, as previously reported.^{10,11} The photocurrent on the CoO_x/TaON electrode was higher than that on the electrode prepared from unloaded TaON particles through the post-necking process at 823 K in NH_3 flow (see Figure 1A-(iii)), while the increase of photocurrent by CoO_x loading was not so significant compared to the case of IrO_2 loading.^{10,11} The onset potentials of unloaded and CoO_x/TaON electrodes were measured to be about -0.05 and -0.25 V vs RHE, respectively.

Figure 1B shows the time courses for the photocurrents of various TaON electrodes at a fixed potential of 0.95 V vs RHE under continuous visible light irradiation. The immediate and rapid decrease in the photocurrent generated by an unloaded TaON electrode (Figure 1B-(i)) can be attributed to self-oxidative deactivation of the TaON surface by photogenerated holes, which reduced nitrogen content, as reported previously.^{10,11} Indeed, the N/Ta atomic ratio determined by XPS analysis decreased significantly from 0.73 to 0.17 after photoirradiation for 1 h. In contrast, the CoO_x/TaON electrode exhibited a stable photocurrent over 60 min (although there is a current spike at the beginning of light irradiation), as shown in Figure 1B-(ii).

The number of electrons passing through the outer circuit in 1 h (16.3 C, corresponding to $169 \mu\text{mol}$ of electrons) exceeded the molar amounts of both TaON (ca. $14.2 \mu\text{mol}$) and CoO_x cocatalyst (ca. $2.5 \mu\text{mol}$, calculated as CoO) in the electrode. As the STEM image of CoO_x/TaON particles peeled from the electrode (Figure 2a) clearly shows, preloading produced highly

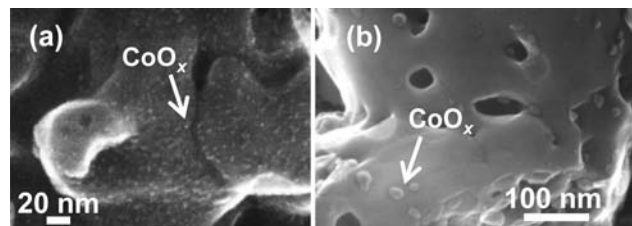


Figure 2. STEM images of (a) $\text{CoO}_x(\text{pre})$ and (b) $\text{CoO}_x(\text{post})/\text{TaON}$ particles peeled from the electrode after the post-necking treatment.

dispersed fine CoO_x particles with diameters of 2–5 nm on the TaON surface, even after the post-necking treatment. The highly dispersed CoO_x nanoparticles efficiently scavenge photogenerated holes and effectively suppress self-oxidation of TaON surfaces, resulting in the stable photocurrent. Indeed, the N/Ta atomic ratio of CoO_x/TaON electrode was almost unchanged after photoirradiation for 1 h. In contrast, the photocurrent of the $\text{CoO}_x(\text{post})/\text{TaON}$ electrode, which was prepared by dropping $\text{Co}(\text{NO}_3)_2$ methanol solution onto the unloaded TaON electrode followed by heating in NH_3 stream, decreased gradually during photoirradiation (see Figure 1B-(iii)). At the same time, the N/Ta ratio decreased appreciably from 0.69 to 0.17 on photoirradiation. As shown in Figure 2b, relatively large ($\sim 20 \text{ nm}$) CoO_x particles were poorly dispersed on the TaON surface, so that a large portion of the TaON surface was uncovered and able to be oxidized during

photoirradiation, resulting in a reduction in the photocurrent even with CoO_x loading, just as for the colloidal IrO_x/TaON electrode reported previously.^{10,11} As shown above, the preloading procedure is a remarkably effective way to homogeneously disperse CoO_x nanoparticles on a TaON surface and to stabilize the photocurrent of the TaON electrode by suppressing self-oxidative deactivation. Since n-type bulk semiconductors generally have a short hole diffusion length, realizing a high dispersion of the CoO_x cocatalyst is essential for efficient hole scavenging. It should be noted that the CoO_x cocatalysts function efficiently even after the post-necking treatment in which TaCl_5 methanol solution was used to treat CoO_x/TaON electrodes prior to testing. As a TEM image of CoO_x/TaON particles (Figure S3) peeled from the electrode shows, most of the CoO_x surface seems to be uncoated, even after the post-necking process. That is, TaCl_5 appears to be preferentially deposited on the TaON surface, instead of the loaded Co species, leaving the CoO_x surface uncoated and enabling it to function as an efficient cocatalyst for water oxidation. We also attempted to prepare IrO_x/TaON electrodes by both pre- and post-loading methods, but the IrO_x/TaON particles could not be deposited by the electrophoretic method; this may be due to the electric charge of the particles being too low in acetone solution. The post-loading of IrO_x on TaON electrode produced poor distributions of fine (2–5 nm) IrO_x particles (see Figure S4) and resulted in an unstable photocurrent (see Figure 1B-(iv)).

Figure 3A shows the time courses of the photocurrent of the CoO_x/TaON electrode in aqueous solutions (pH 8) containing

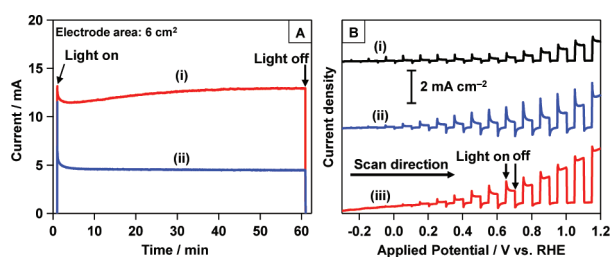


Figure 3. (A) Time courses of the photocurrent of CoO_x/TaON electrode in aqueous (i) sodium phosphate buffer and (ii) Na_2SO_4 solutions (pH 8) at 1.07 V vs RHE under visible light irradiation ($\lambda > 400$ nm). (B) Current–potential curves under chopped visible light irradiation ($\lambda > 400$ nm) for (i) unloaded TaON in aqueous Na_2SO_4 (pH 8), (ii) CoO_x/TaON in aqueous Na_2SO_4 (pH 8), and (iii) CoO_x/TaON in aqueous sodium phosphate buffer solution (pH 8).

Na_2SO_4 or phosphate (PO_4^{3-}) electrolyte (0.1 M) at 1.07 V vs RHE under visible light irradiation. The photocurrent of CoO_x/TaON was considerably higher when the phosphate electrolyte solution was used. Kanan and Nocera have reported that an amorphous cobalt/phosphate phase, prepared by in situ anodic polarization of an inert electrode such as ITO in the presence of Co^{2+} and phosphate ions, can function as a highly efficient catalyst for water oxidation.¹² XPS analysis indicates that the CoO_x/TaON electrode after the photoreaction in phosphate aqueous solution contained an appreciable amount of phosphorus even after careful washing. The P/Ta ratio (0.28) after photoirradiation with an applied potential of 1.07 V was much higher than after applying the same potential in the dark (0.11) or after leaving the electrode in the solution in the dark (0.11). These results indicate that composite phases of Co and P (Co–P) were produced by a photoelectrochemical

process, involving the reaction with photogenerated holes in TaON. Such photoelectrochemical deposition of Co–P composite on $\alpha\text{-Fe}_2\text{O}_3$ photoanode has also been reported by Zhong et al.¹³ Although the role of phosphate in Co–P systems is not fully understood as yet, the Co–P does indeed enhance the efficiency of water photo-oxidation when coupled with various metal oxide photoanodes, such as WO_3 ¹⁴ and $\alpha\text{-Fe}_2\text{O}_3$.¹⁵ It has been generally considered that such Co–P species loaded on photoanodes primarily function as an efficient catalyst for water oxidation, like the well-known IrO_2 ,¹⁶ RuO_2 ,¹⁷ Co_3O_4 ,¹⁸ or MnO_x .^{19,20}

Durrant et al. recently suggested another key role of Co–P species loaded on $\alpha\text{-Fe}_2\text{O}_3$ photoanode, based on the results of transient absorption spectroscopy. It was proposed that the enhanced photoelectrochemical activity of Co–P/ $\alpha\text{-Fe}_2\text{O}_3$, and in general $\text{CoO}_x/\alpha\text{-Fe}_2\text{O}_3$ composite photoanode, for water oxidation resulted from the reduced recombination between electrons and holes due to the formation of a Schottky-type heterojunction between them.²¹ In the present CoO_x/TaON photoanode system, the photocurrent densities in the negative potential region (–0.2–0.4 V vs RHE) were appreciably increased by the loading of CoO_x species on bare TaON (Figure 3B). The sharp anodic current spikes and cathodic transient peaks were notably observed on CoO_x/TaON when the light irradiation was turned on and off, respectively, in an aqueous Na_2SO_4 solution. These indicate that the photogenerated holes in TaON bulk efficiently transfer to CoO_x through the heterojunction when the light reaches the sample, but most of them accumulate without reacting with water molecules due to the insufficient catalytic activity of CoO_x surface, which results in the enhanced recombination with electrons. On the other hand, the use of CoO_x/TaON in phosphate (PO_4^{3-}) electrolyte solution significantly suppressed such a sharp current decay. Increased photocurrent densities were observed throughout the potential region, as shown in Figure 3B. Clearly, the Co–P species possess higher catalytic activity for water oxidation than CoO_x , but one cannot entirely exclude the possibility that the heterojunctions between Co–P and TaON retard the recombination more effectively than those between CoO_x and TaON. One possible explanation is that the CoO_x phase inside mainly functions to retard the charge recombination in the TaON bulk, and the Co–P phase formed outside of CoO_x works as an efficient catalyst for water oxidation. Although the fine structure of CoO_x (and Co–P) and their functions on TaON need further investigation, we have demonstrated that the phosphorized Co cocatalyst is effective in enhancing water oxidation on oxynitrides, such as TaON. The incident photon-to-charge carrier efficiency (IPCE) of the CoO_x/TaON electrode was calculated to be ca. 42% at 400 nm at 1.2 V vs RHE in sodium phosphate buffer solution (pH 8), which is lower than that of colloidal IrO_x/TaON electrode (ca. 76% at 400 nm at 1.15 V vs RHE in aqueous Na_2SO_4 solution) obtained in our previous studies.^{10,11} However, the photocurrent of the IrO_x/TaON electrode was decreased remarkably after 60 min to one-third of its initial value.^{10,11} It is therefore concluded that the CoO_x/TaON electrode fabricated in the present study is superior to the IrO_x/TaON system in terms of practical applications for which electrodes with long stabilities are strongly desired.

H_2 and O_2 were evolved at close to the expected stoichiometric ratio under the same conditions as those in Figure 3A-(i) (see Figure 4). The amounts of gases evolved in 150 min (H_2 , 336 μmol ; O_2 , 167 μmol) were considerably

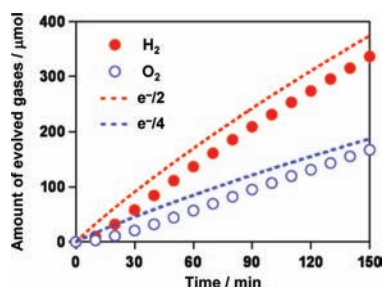


Figure 4. Time courses of gas evolution for CoO_x/TaON electrode in aqueous sodium phosphate buffer solution (pH 8) at 1.07 V vs RHE under visible light irradiation ($\lambda > 400$ nm).

higher those for TaON (ca. 14.2 μmol). The amount of H₂ evolved was slightly less than half of the electrons passing through the outer circuit ($e^-/2$, indicated by the broken line) due to water formation from H₂ and O₂ (i.e., the undesired backward reaction) on the Pt electrode. We also found that H₂ and O₂ are simultaneously evolved in sodium phosphate buffer solution (pH 8) with an applied bias of >0.6 V between the CoO_x/TaON working electrode and Pt counter electrode (with no reference), as shown in Figure S5.

This is the first demonstration of stable photoelectrochemical splitting of water into H₂ and O₂ on an oxynitride photoanode under visible light with a high IPCE and a high current efficiency. The preloading of CoO_x cocatalyst on TaON particles produced a hybrid material with highly dispersed CoO_x nanoparticles that are efficient hole scavengers and effectively suppressed self-oxidative deactivation processes, even after electrophoretic deposition and subsequent post-necking treatment. The combination of highly dispersed CoO_x cocatalyst on TaON with phosphate solutions significantly increased the photocurrent due to the formation of composite phases of Co and P that remarkably enhance water oxidation. Although further improvements of CoO_x/TaON photoanodes (especially reducing the resistance of the TaON photoanode) are necessary to achieve highly efficient water splitting at a lower applied bias, the present study demonstrates the potential of oxynitride semiconductors as stable photoanodes when used with an appropriate cocatalyst for water oxidation.

■ ASSOCIATED CONTENT

📄 Supporting Information

XPS spectra, TEM image, and current–potential curves of CoO_x/TaON electrode, and photoelectrochemical water splitting result. This material is available free of charge via the Internet at <http://pubs.acs.org>.

■ AUTHOR INFORMATION

Corresponding Author

ryu-abe@cat.hokudai.ac.jp

Notes

The authors declare no competing financial interest.

■ ACKNOWLEDGMENTS

This work was supported by the Development in a New Interdisciplinary Field Based on Nanotechnology, Materials Science program of the Ministry of Education, Culture, Sports, Science and Technology (MEXT) of Japan, CREST-JST Program, and The KAITEKI Institute, Inc.

■ REFERENCES

- (1) Maeda, K.; Domen, K. *J. Phys. Chem. C* **2007**, *111*, 7851–7861.
- (2) Kudo, A.; Miseki, Y. *Chem. Soc. Rev.* **2009**, *38*, 253–278.
- (3) Esswein, M. J.; Nocera, D. G. *Chem. Rev.* **2007**, *107*, 4022–4047.
- (4) Abe, R. *J. Photochem. Photobiol. C* **2010**, *11*, 179–209.
- (5) Santato, C.; Ulmann, M.; Augustynski, J. *J. Phys. Chem. B* **2001**, *105*, 936–940.
- (6) Kay, A.; Cesar, I.; Gratzel, M. *J. Am. Chem. Soc.* **2006**, *128*, 15714–15721.
- (7) Sayama, K.; Nomura, A.; Arai, T.; Sugita, T.; Abe, R.; Yanagida, M.; Oi, T.; Iwasaki, Y.; Abe, Y.; Sugihara, H. *J. Phys. Chem. B* **2006**, *110*, 11352–11360.
- (8) Hitoki, G.; Takata, T.; Kondo, J. N.; Hara, M.; Kobayashi, H.; Domen, K. *Chem. Commun.* **2002**, 1698–1699.
- (9) Chun, W. J.; Ishikawa, A.; Fujisawa, H.; Takata, T.; Kondo, J. N.; Hara, M.; Kawai, M.; Matsumoto, Y.; Domen, K. *J. Phys. Chem. B* **2003**, *107*, 1798–1803.
- (10) Abe, R.; Higashi, M.; Domen, K. *J. Am. Chem. Soc.* **2010**, *132*, 11828–11829.
- (11) Higashi, M.; Domen, K.; Abe, R. *Energy Environ. Sci.* **2011**, *4*, 4138–4147.
- (12) Kanam, M. W.; Nocera, D. G. *Science* **2008**, *321*, 1072–1075.
- (13) Zhong, D. K.; Cornuz, M.; Sivula, K.; Gratzel, M.; Gamelin, D. R. *Energy Environ. Sci.* **2011**, *4*, 1759–1764.
- (14) Seabold, J. A.; Choi, K. S. *Chem. Mater.* **2011**, *23*, 1105–1112.
- (15) Zhong, D. K.; Gamelin, D. R. *J. Am. Chem. Soc.* **2010**, *132*, 4202–4207.
- (16) Hara, M.; Waraksa, C. C.; Lean, J. T.; Lewis, B. A.; Mallouk, T. E. *J. Phys. Chem. A* **2000**, *104*, 5275–5280.
- (17) Fang, Y. H.; Liu, Z. P. *J. Am. Chem. Soc.* **2010**, *132*, 18214–18222.
- (18) Harriman, A.; Pickering, I. J.; Thomas, J. M.; Christensen, P. A. *J. Chem. Soc., Faraday Trans. 1* **1988**, *84*, 2795–2806.
- (19) Brimblecombe, R.; Koo, A.; Dismukes, G. C.; Swiegers, G. F.; Spiccia, L. *J. Am. Chem. Soc.* **2010**, *132*, 2892–2894.
- (20) Hocking, R. K.; Brimblecombe, R.; Chang, L. Y.; Singh, A.; Cheah, M. H.; Glover, C.; Casey, W. H.; Spiccia, L. *Nature Chem.* **2011**, *3*, 461–466.
- (21) Barroso, M.; Cowan, A. J.; Pendlebury, S. R.; Gratzel, M.; Klug, D. R.; Durrant, J. R. *J. Am. Chem. Soc.* **2011**, *133*, 14868–14871.